2006

Measurements and modeling of optical turbulence in a maritime environment

Frederickson, Paul A.

Measurements and modeling of optical turbulence in a maritime environment

Paul A. Frederickson[*a], Stephen Hammel[b], and Dimitris Tsintikidis[b]
[a]Department of Meteorology, Naval Postgraduate School, Monterey, CA
[b]Space and Naval Warfare Systems Center, San Diego, CA

ABSTRACT

Turbulence can be a dominant factor in image and laser beam degradation for optical systems operating in the near-surface maritime environment. A long-term propagation field experiment was conducted at Zuniga Shoal (near San Diego) to study the impact of environmental conditions on low-altitude laser propagation above the ocean surface. Test periods of one month duration were conducted at various points of the year, during which scintillometer measurements were obtained along a 7.2 km over-water path and a 'flux' research buoy deployed along the propagation path collected concurrent mean meteorological, atmospheric turbulence, and wave data.

We use the refractive index structure parameter (C_n^2) as the critical parameter for quantifying the effects of atmospheric turbulence on laser system performance, including received power fluctuations, beam spread and beam wander. Bulk estimates of C_n^2 were derived from the buoy mean meteorological measurements using the Navy Surface Layer Optical Turbulence (NSLOT) model. C_n^2 was also determined from atmospheric turbulence measurements obtained from a sonic anemometer on the buoy. These independent C_n^2 values derived from the buoy data are compared with C_n^2 values computed from the infrared propagation measurements to determine how the NSLOT model performs under different environmental conditions. In addition, the optical measurements and bulk estimates of C_n^2 are used to study the effects of the atmospheric turbulence on operational optical systems.

Keywords: scintillation, optical turbulence, refractive-index structure parameter (C_n^2), bulk models

1. INTRODUCTION

In the past several decades, much effort has been put into developing models to describe atmospheric optical turbulence from mean atmospheric measurements. Optical turbulence is often quantified through the refractive index structure parameter, C_n^2. Important optical turbulence effects on imaging and laser systems, such as image blurring, received signal intensity variations, beam wander and beam spread, are related to C_n^2. Since direct measurements of C_n^2 over the ocean are difficult and expensive to obtain, it is useful to be able to estimate C_n^2 from routinely measured environmental parameters. Bulk models have been developed to estimate near surface C_n^2 values from mean meteorological and sea temperature measurements, which can be made relatively easily from ships, buoys and ocean towers. Important uses of bulk C_n^2 models include the ability to predict C_n^2 values from numerical weather prediction model outputs, to construct C_n^2 climatologies from historical marine meteorological data bases, and to use real-time, in situ meteorological measurements to produce C_n^2 estimates to assist operational personnel in optimally employing their EO systems in the current environment.

The goal of this study is to use a large data set obtained during a recent propagation field experiment conducted in the Zuniga Shoals area near San Diego in May 2005 to gain a better understanding of how C_n^2 behaves with different environmental conditions and to use this understanding to improve current bulk models for estimating C_n^2 from mean atmospheric measurements. Environmental measurements obtained from a buoy are compared with concurrent single-point turbulence C_n^2 values and optical scintillation-derived C_n^2 measurements obtained along an over-water propagation path to determine how C_n^2 varies with different environmental parameters. Bulk model versus turbulent and scintillation C_n^2 comparisons are also conducted to identify potential model improvements.

[*]E-mail: pafreder@nps.edu; Telephone: 831 656 2407; Fax: 831 656 3061

2. THEORETICAL BACKGROUND

The turbulent fluctuation component of the refractive index of air, n, can be expressed to a first order approximation as a function of turbulent air temperature and specific humidity fluctuations, as follows[1]:

$$n' = A(\lambda, P, T, q)T' + B(\lambda, P, T, q)q' \tag{1}$$

where

$$A = \frac{\partial n}{\partial T} = -10^{-6}\frac{P}{T^2}\left\{m_1(\lambda) + \left[m_2(\lambda) - m_1(\lambda)\right]\frac{q}{\varepsilon\gamma}\right\}, \tag{2}$$

$$B = \frac{\partial n}{\partial q} = 10^{-6}\left[m_2(\lambda) - m_1(\lambda)\right]\frac{P}{T\varepsilon\gamma^2}. \tag{3}$$

and λ is the optical wavelength, P is atmospheric pressure, T is the air temperature, q is specific humidity, $\varepsilon = 0.622$, and $\gamma = (1 + 0.61q)$. m_1 and m_2 are empirical functions of wavelength. For the wavelength we will be examining in this study, 1.62 μm, $m_1 = 77.66$ and $m_2 = 65.09$.

Within the inertial-subrange of the atmospheric turbulence spectrum, the refractive index structure parameter, C_n^2, is defined as:

$$C_n^2 = \frac{\overline{\left[n'(0) - n'(r)\right]^2}}{r^{2/3}}, \tag{4}$$

where $n'(0)$ and $n'(r)$ are the turbulent fluctuation values of n at two points separated by a distance r along the mean wind direction and the overbar denotes an ensemble average. In practice r is generally taken to be on the order of roughly 10 cm, therefore C_n^2 as defined by Eq. (4) is a statistical description of small-scale refractive index fluctuations. C_n^2 can also be expressed in terms of the structure parameters for temperature, C_T^2, specific humidity, C_q^2 and the temperature-specific humidity cross-structure parameter, C_{Tq}, all defined similar to Eq. 4, as follows[1]:

$$C_n^2 = A^2C_T^2 + 2ABC_{Tq} + B^2C_q^2. \tag{5}$$

The first term on the right-hand side of Eq. (5) represents refractive index fluctuations caused by temperature fluctuations and is always positive, the second term represents the correlation of temperature and humidity fluctuations and can be positive or negative, while the third term represents humidity fluctuations and is always positive.

C_n^2 values can also be determined by optical systems from the normalized variance of the measured intensity fluctuations in a signal that has propagated through the turbulent atmosphere, σ_I^2, using the generalized relation:

$$C_n^2 = 2\sigma_I^2\left(\frac{2\pi}{\lambda}\right)^{-7/6}L^{-11/6}F \tag{6}$$

where λ is the optical wavelength, L is the propagation path length and F is a dimensionless function which incorporates the effects of the turbulence strength and aperture averaging for finite size incoherent source and receiver apertures.

Equations (4-5) and (6) represent two very different means of determining C_n^2. Equations (4-5) are for single-point atmospheric turbulence measurements which are highly dependent upon the specific height above the surface and horizontal point in space where the measurements are taken, whereas Eq. (6) is a path-averaged measurement which includes the effects of horizontal variations in atmospheric turbulence along the path and also variations in turbulence levels at different heights above the surface as the optical rays are refracted through the atmosphere. We would expect the two methods to agree best when atmospheric conditions approach horizontally homogeneity

3. THE BULK C_n^2 MODEL

Near the surface, Monin-Obukhov similarity theory (MOST) can be used to relate the structure parameters C_T^2, C_q^2 and C_{Tq} in Eq. (5) to the mean properties of the atmospheric surface layer. According to MOST, conditions are assumed to be horizontally homogeneous and stationary; the turbulent fluxes of momentum, sensible heat and latent heat are assumed to be constant with height in the surface layer; and all dynamical properties within the surface layer, when scaled by the proper parameters, are assumed to be a dimensionless function of ξ, defined as:

$$\xi = \frac{z}{L_{MO}} = \frac{zkg(\theta_* + 0.61Tq_*)}{\theta_v u_*^2}, \tag{7}$$

where z is the height above the surface, L_{MO} is the Monin-Obukhov length scale, k is the von Karman constant (= 0.4) and T_*, q_* and u_* are the scaling parameters for temperature, humidity and wind speed, respectively. The ratio ξ is often referred to simply as the 'stability', and is negative in unstable conditions, zero in neutral conditions, and positive in stable conditions. The surface layer scaling parameters can be expressed as:

$$x_* = (\Delta x)k[\ln(z / z_{ox}) - \psi_x(\xi)]^{-1}, \tag{8}$$

where x represents wind speed (u), temperature (T) or specific humidity (q) and the symbol Δ denotes the mean air-sea difference. The ψ functions are the integrated dimensionless profile functions. We have made the common assumption that $\psi_T = \psi_q$. The parameters z_{ou}, z_{oT} and z_{oq} are known as the 'roughness lengths,' and are determined by the bulk surfaced-layer model formulated by Fairall et al.[2].

The structure parameters for temperature (C_T^2) and specific humidity (C_q^2) and the temperature-specific humidity cross-structure parameter (C_{Tq}) can be expressed in terms of the surface layer scaling parameters as follows:

$$C_T^2 = T_*^2 z^{-2/3} f_T(\xi), \tag{9a}$$

$$C_{Tq} = r_{Tq} T_* q_* z^{-2/3} f_{Tq}(\xi), \tag{9b}$$

$$C_q^2 = q_*^2 z^{-2/3} f_q(\xi), \tag{9c}$$

where r_{Tq} is the temperature-specific humidity correlation coefficient with a value of about 0.8, and f_T, f_{Tq}, and f_q are dimensionless functions of ξ that have been determined empirically, as follows[1]:

$$f_T(\xi) = f_q(\xi) = \begin{cases} 5.9(1-8\xi)^{-2/3}, & \xi \le 0 \\ 5.9(1+2.4\xi^{2/3}), & \xi \ge 0 \end{cases}. \tag{10}$$

We can express C_n^2 in terms of mean meteorological properties by combining Eqs. (5, 7-10), resulting in:

$$C_n^2 = \frac{f(\xi)k^2\left[A^2\Delta T^2 + 2ABr_{Tq}\Delta T\Delta q + B^2\Delta q^2\right]}{z^{2/3}\left[\ln(z / z_{oT}) - \Psi_T(\xi)\right]^2}. \tag{11}$$

and

$$\xi = \frac{zg(\Delta\theta + 0.61T\Delta q)\left[\ln(z / z_{oU}) - \Psi_U(\xi)\right]^2}{\theta_v(\Delta U)^2\left[\ln(z / z_{oT}) - \Psi_T(\xi)\right]}. \tag{12}$$

Once the required model inputs (ΔT, Δq, ΔU) are known, C_n^2 can be estimated by solving Eqs. (11-12) by an iterative process. Full details on the Naval Postgraduate School's bulk C_n^2 model are provided by Frederickson et al (2000)[3].

The dependence of the bulk C_n^2 estimates on the air – sea temperature difference (ΔT) is shown as a function of wind speed and relative humidity in Figs. 1a and 1b, respectively. The C_n^2 estimates generally increase as $|\Delta T|$ increases. The C_n^2 estimates increase with wind speed for negative ΔT values, and generally decrease with wind speed when ΔT is positive. Wind speed variations have the largest effect on C_n^2 for large $|\Delta T|$ values and are slightly larger when $\Delta T < 0$. The bulk C_n^2 estimates decrease with relative humidity for negative ΔT values and generally increase with relative humidity when ΔT is positive. The minimum C_n^2 values increase and occur at larger ΔT values as relative humidity decreases. The effects of relative humidity variations on the bulk C_n^2 estimates are largest for small $|\Delta T|$ values.

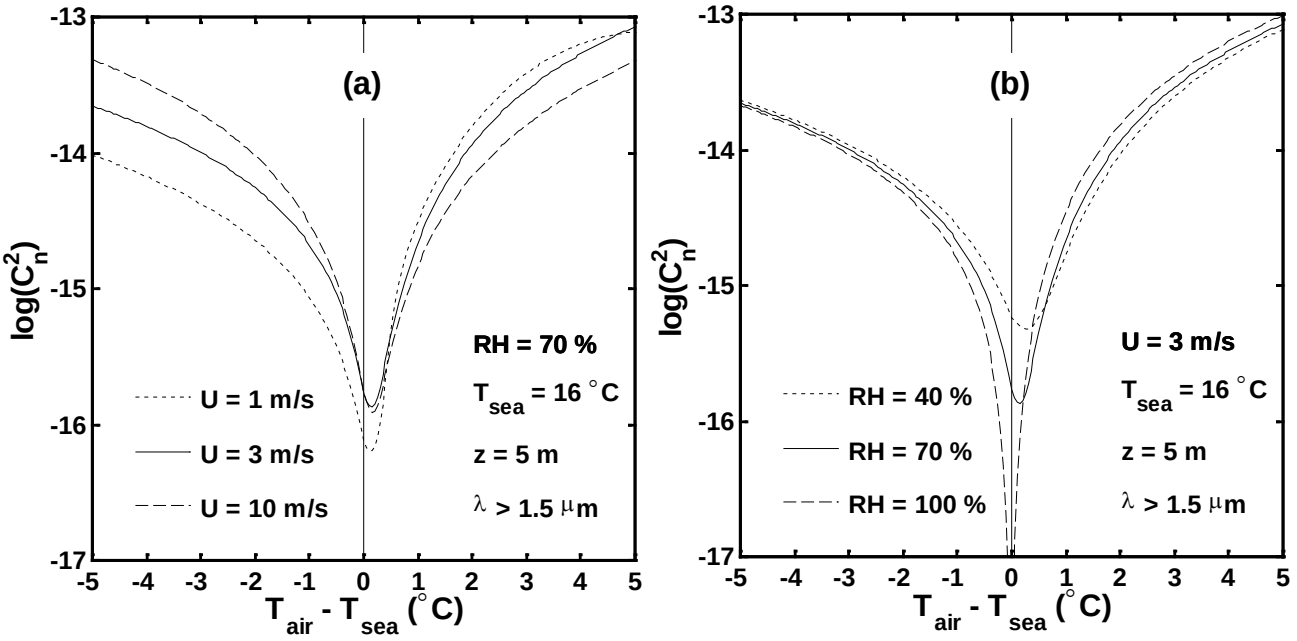

Figure 1. Bulk estimates of $\log(C_n^2)$ versus air – sea temperature difference, (a) plotted for different values of wind speed (U) as indicated; and (b) plotted for different values of relative humidity (RH) as indicated. The bulk C_n^2 estimates were computed for a sea temperature of 16 °C, height above the ocean surface of 5 m, and a wavelength of 1.62 μm.

4. THE EXPERIMENTS

During 2005, four Intensive Observation Periods (IOPs) of one-month duration were conducted as part of the Navy Atmospheric Propagation Measurements field campaign. During these IOPs low-level infrared scintillation measurements were obtained by the SPAWAR Systems Center, San Diego (SSC-SD) along a propagation path over the Zuniga Shoals outside of San Diego Bay, while concurrent meteorological and ocean surface measurements were collected by the Naval Postgraduate School's (NPS) buoy, located along the propagation path (see Fig. 2). Measurements of wind speed, wind direction, air temperature, relative humidity, atmospheric pressure and sea temperature are obtained every second on the buoy. These 1 Hz data were then averaged over 15 minute intervals centered about the scintillation measurement times and bulk C_n^2 estimates were computed from these averaged values. Since C_n^2 is height dependent, the bulk C_n^2 estimates were adjusted

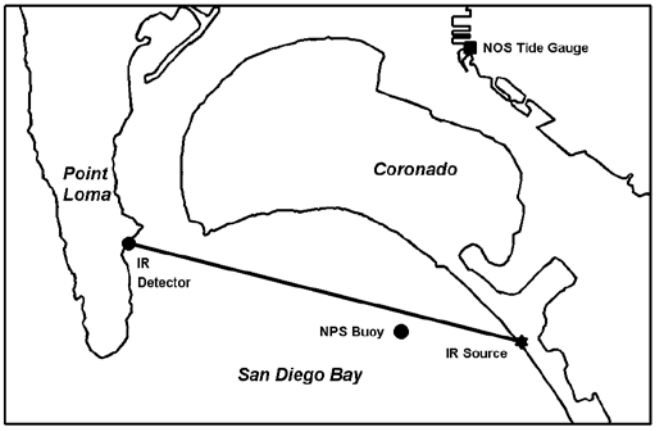

Figure 2. Map of the experiment area, showing locations of the measurement platforms and the 7.2 km propagation path.

for tidal sea level variations using tide data obtained from the National Ocean Service acoustic tide gauge located in San Diego Harbor.

High frequency (10 Hz) sonic temperature measurements were obtained on the NPS buoy from a Solent sonic anemometer mounted 5.25 m above the waterline. The sonic temperature structure parameter, $C_{T_s}^2$, was computed from power spectral densities of the sonic temperature, $S_{T_s}(f)$, using the expression:

$$C_{T_s}^2 = 4\left(\frac{2\pi}{U}\right)^{2/3} S_{T_s}(f) f^{5/3}, \tag{13}$$

where U is the mean wind speed and f is the frequency. Direct turbulent estimates of C_n^2 were obtained from the relationship $C_n^2 = A^2 C_{T_s}^2$, which assumes that humidity fluctuation effects on both $C_{T_s}^2$ and C_n^2 are negligible compared to temperature fluctuations.

The dimensionless temperature structure parameter function (f_T) was also computed from turbulence measurements obtained on the NPS buoy. This dimensionless function is derived simply by scaling the temperature structure parameter C_T^2 by the relevant MOST surface layer scaling parameters (in this case T_* and z), as follows:

$$f_T = \frac{C_T^2 z^{2/3}}{T_*^2} \tag{14}$$

The temperature scaling parameter, T_*, was determined from the NPS buoy measurements by the direct covariance method. First, the buoy motion was removed from the sonic anemometer wind measurements, using data obtained from the onboard motion sensor. Next, the covariance of the vertical wind component and temperature fluctuations was computed (<w'T'>) and the wind speed scaling parameter (u_*), often referred to as the 'friction velocity', was determined. The temperature scaling parameter T_* could then be computed using the relation:

$$T_* = -\frac{< u'T' >}{u_*} \tag{15}$$

Once C_T^2 and T_* were determined, f_T is computed using Equation (14).

Infrared (IR) scintillation measurements were obtained by SSC-SD every 15 minutes, when the amplitude of an infrared signal was recorded at a 300 Hz rate for a 109 second period in two wavelengths; near IR (1.06 μm) and short-wave IR (1.62 μm). The broad-beam IR transmitting source consists of 18 halogen lamps mounted inside a circle 25 cm in diameter and modulated by a 690 Hz chopper wheel. The receiver system consists of a telescope with a 20 cm diameter primary mirror, a beam splitter that separates the incoming beam to two 3 mm diameter photodiode detectors, one for each wavelength. A reference signal from the chopper blade is transmitted by radio to a synchronous detector at the receiver. The signal from the detectors is separated from the chopped carrier waveform by means of a lock-in amplifier system. C_n^2 values were calculated from the normalized variance of the measured signal amplitude, using a specialized form of Eq. (6), which takes into account the effects of aperture averaging. For more details on the SSC-SD equipment and procedures, see Zeisse et al. (2000)[4]. The transmitting source is located at the Naval Amphibious Base, Coronado, California, at a height of ~6.5 m above mean sea level (see Fig. 2). The receiver is located 7.2 km from the transmitter at the Submarine Base, Point Loma, California, at a height of ~11.5 m above mean sea level. The transmission path is over-water for its entire length except for very short distances at each end point.

5. RESULTS

In this study we will examine data obtained during the May and August 2005 Intensive Observation Periods (IOPs) at Zuniga Shoals. Although data for two wavelengths was collected, only data for 1.62 μm will be shown here,

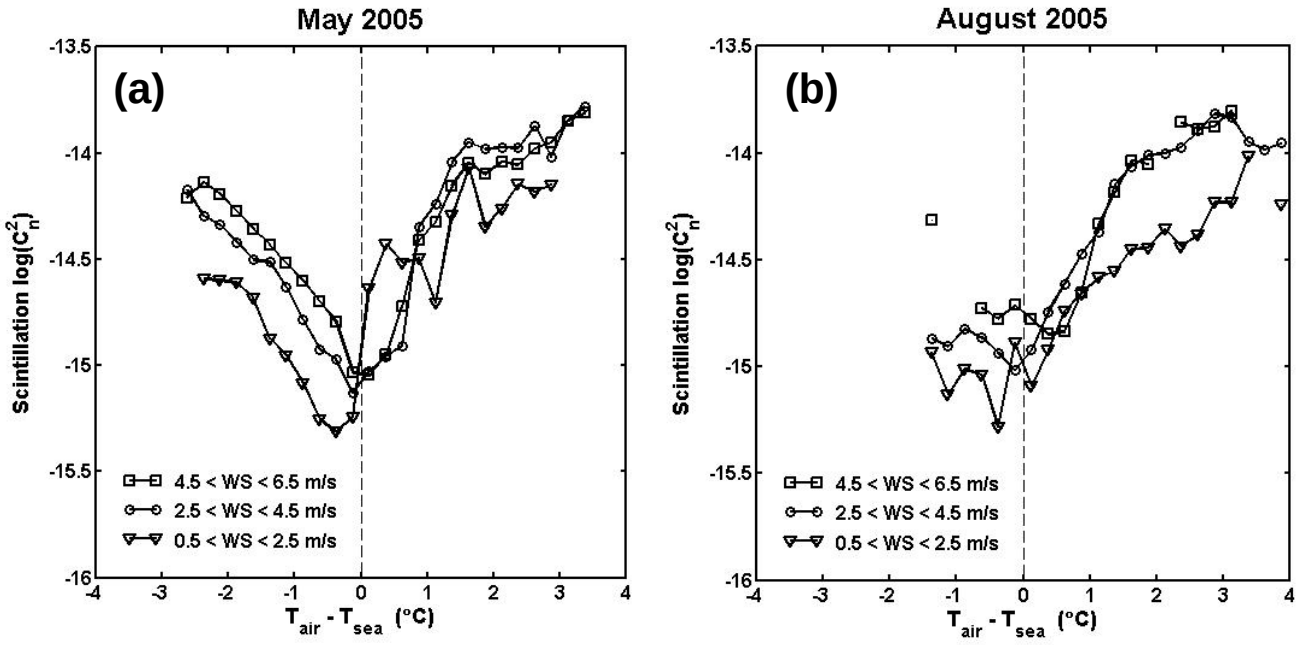

Figure 3. Scintillation $\log_{10}(C_n^2)$ values plotted versus the air-sea temperature difference for different wind speed regimes, as indicated, and for: (a) May 2005, and (b) August 2005. The data have been averaged into air-sea temperature difference bins.

since the results at 1.06 and 1.62 μm were nearly identical. An initial study of the behavior of the scintillation and buoy turbulent C_n^2 values as a function of the environmental conditions observed at the buoy was reported earlier by Frederickson et al. (2005)[5]. In this previous study a definite wind speed dependence of C_n^2 upon wind speed was observed in unstable conditions (negative air-sea temperature difference), as shown in Fig. 3a. Data from the August 2005 are shown in Fig. 3b. This data indicate that in stable conditions (positive air-sea temperature difference) low wind speed conditions correspond to much lower C_n^2 values, unlike what was observed in the May 2005 data. Other than this discrepancy, the data from the two IOPs appear to be very similar.

We further isolated different environmental cases to try to identify other potential relationships between C_n^2 and environmental conditions. Most of these attempts, such as examining variations in C_n^2 due to relative humidity variations, did not result in any discernable relationship. In Fig. 4 we separated the data into cases with the wind blowing from the direction of the open sea and the wind blowing from over the nearby land surfaces. Since the propagation path and the NPS buoy were located so close to the shore, it seemed possible that there could be a difference in the behavior of C_n^2 for these two cases, since the air mass causing refractive index fluctuations would have a history of being influenced by surfaces with very different properties. From Fig. 4, however, we can see very little difference in the C_n^2 versus ASTD comparisons for the onshore and offshore wind cases. High winds occurred almost exclusively during periods with afternoon sea breeze, therefore there is very little data in the "wind from land" case with higher winds, making comparisons impossible.

We also examined possible impacts of surface waves on C_n^2. It is known that waves can induce vertical mixing in the lower part of the atmospheric surface layer. This mixing can have the effect of decreasing vertical gradients of atmospheric properties. Since this effect is not taken into account in current bulk models, it seems to follow that if such mixing were actually occurring, the bulk C_n^2 estimates should be higher than the actual scintillation C_n^2 measurements, which is what is observed in stable conditions[5]. The relationship between C_n^2 and ASTD is shown for lower and higher wave conditions, in terms of significant wave height measured by the NPS buoy, in Fig. 5. Very little difference between the two wave cases can be observed. The significant wave height only varied between 0.5 and 1.5 m in our data set, therefore it is possible that there is no discernable dependence of C_n^2 on waves because the variation in wave conditions was too small. Probably the more likely explanation, however, is that the propagation took place at heights

too high above the surface (the lowest end of the propagation path was at ~6.5 m height) for waves with heights less than 1.5 m to induce significant mixing.

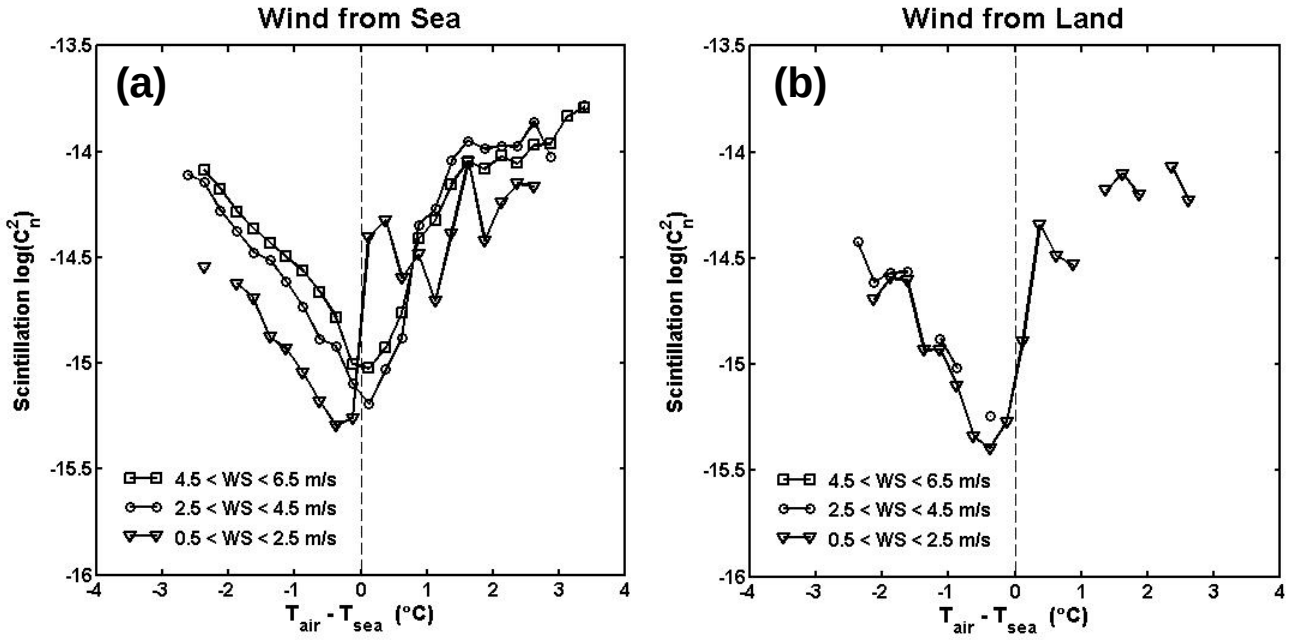

Figure 4. Scintillation $\log_{10}(C_n^2)$ values plotted versus the air-sea temperature difference for different wind speed regimes, as indicated, for: (a) cases with the wind blowing from the direction of the open sea, and (b) cases with the wind blowing from the direction of the nearby land. The air-sea temperature difference and wind direction data are from the NPS buoy. The C_n^2 data have been averaged into air-sea temperature difference bins.

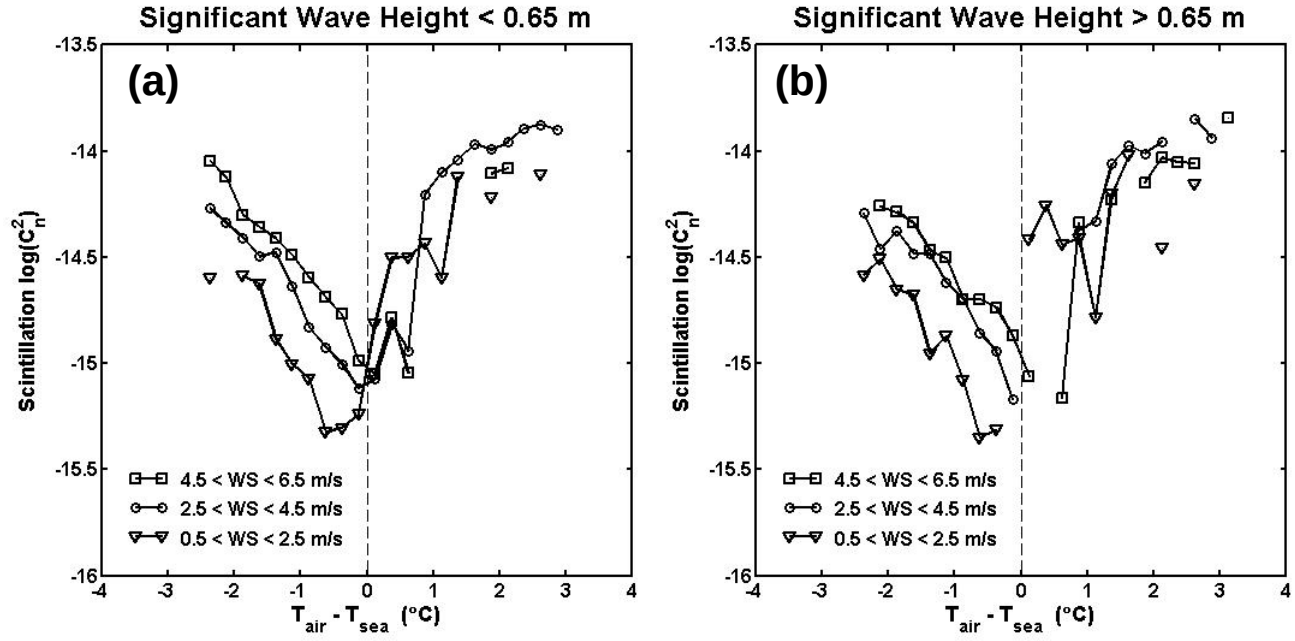

Figure 5. Scintillation $\log_{10}(C_n^2)$ values plotted versus the air-sea temperature difference for different wind speed regimes, as indicated, for: (a) cases with significant wave height (H_s) less than 0.65 m, and (b) cases with H_s greater than 0.65 m. The data have been averaged into air-sea temperature difference bins.

In the Frederickson et al. (2005)[5] study it was noted that the mean differences between bulk estimates and turbulent measurements of C_T^2 for the May 2005 IOP, when plotted as a function of the air-sea temperature difference, exhibited a dependence upon the wind speed for $\Delta T < -1$ °C, as seen in Fig 7a. This indicates that the dimensionless temperature structure parameter (f_T) used to compute the bulk values may be incorrect, since wind speed is the dominant factor in determining the magnitude of f_T (notice that U^2 appears in the denominator of the expression for ξ in Eq. 12). According to MOST, this dimensionless function should be a function only of z/L. Fortunately, f_T can be determined from the turbulence measurements obtained on the NPS buoy. The resulting f_T values computed from the buoy measurements for unstable conditions ($z/L < 0$) are shown in Fig. 6. We can readily see that the Edson (1998)[6] function for f_T does not adequately describe our buoy data. A new function, using the same form as the Edson function but with different constants, was derived to better fit the NPS buoy f_T data in unstable conditions, as follows:

$$f_T = 20\left(1-140\xi\right)^{-2/3} \tag{16}$$

This new f_T function was then used to re-compute bulk C_T^2 values from the mean NPS buoy data, which were again compared with the turbulent C_T^2 values in Fig. 7b. Not surprisingly, the agreement between the bulk and turbulent C_T^2 values was much better in unstable conditions with the new Zuniga Shoals function and, significantly, the air-sea temperature difference and wind speed dependence of the bulk-turbulent difference was virtually eliminated, as seen in Fig. 7b. Like all empirical parameterizations, this new function must be tested further with data sets from other experiments conducted in different geographical areas and with different measurement systems before we can assume it has universal applicability.

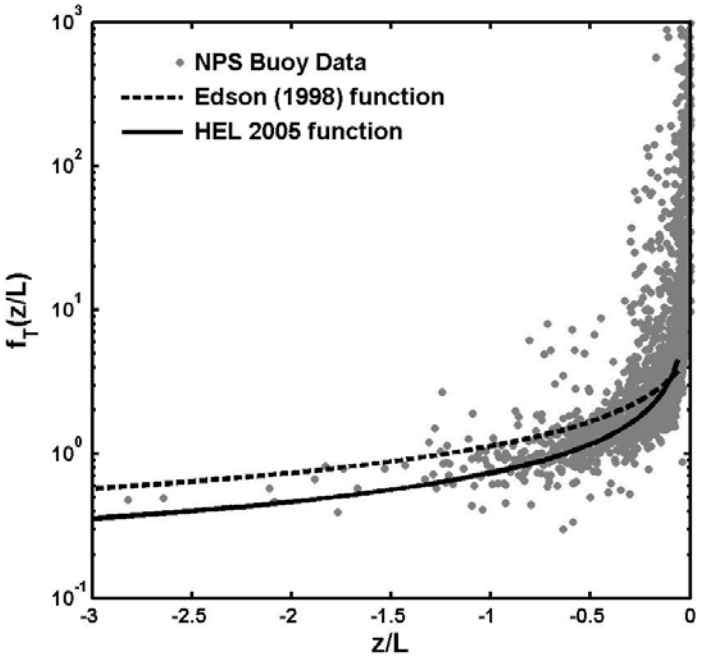

Figure 6. The dimensionless temperature structure parameter (f_T) plotted versus the 'stability', z/L, for unstable conditions ($z/L < 0$). Grey dots are f_T valued computed from the NPS buoy data, the dashed line is the Edson (1998) f_T function (Eq. 10), the solid line is the new Zuniga Shoals 2005 f_T function (Eq. 16).

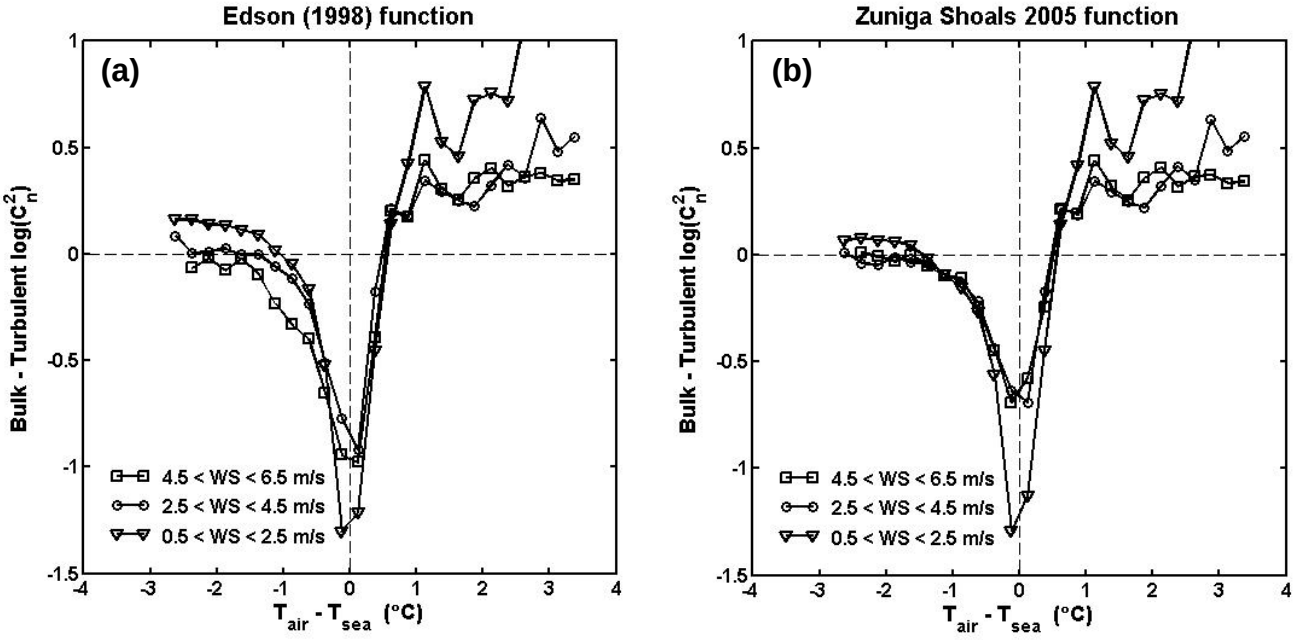

Figure 7. Bulk – Turbulent C_n^2 values derived from the NPS buoy measurements versus the air-sea temperature difference: (a) Bulk C_n^2 values computed using the Edson (1998) dimensionless temperature structure parameter function (f_T) (Eq. 10); (b) Bulk C_n^2 values computed using the new Zuniga Shoals 2005 f_T function (Eq. 16). Data have been averaged into air-sea temperature difference bins and are computed for different wind speed intervals, as indicated.

6. CONCLUSIONS

In this study we have examined the behavior of scintillation-derived C_n^2 values under specific environmental conditions. As expected, a strong correlation between C_n^2 and the air-sea temperature difference (ASTD) was observed in the data, and a clear increase of C_n^2 with wind speed in unstable conditions was noted. Other than these relationships, very little dependence of C_n^2 on other environmental parameters was evident. This is probably due to any actual dependence of C_n^2 on environmental factors other than ASTD and wind speed being too small to resolve when compared to C_n^2 variations caused by horizontal inhomogeneities in the atmospheric and surface properties along the propagation path. Another possibility was that other relationships were lost amidst the measurement noise.

The air-sea temperature difference and wind speed dependence of the bulk-scintillation C_n^2 difference in unstable conditions indicated that the dimensionless stability functions used in the bulk model may be incorrect, since ASTD and wind speed determine the sign and magnitude of z/L. A new dimensionless temperature structure parameter function (f_T) in unstable conditions ($z/L < 0$) was developed from measurements obtained on the NPS buoy in the Zuniga Shoals area. When bulk C_n^2values were computed using the new f_T function, the resulting comparison with turbulent-derived C_n^2 values was much improved and the ASTD and wind speed dependence previously observed in the bulk-turbulent C_n^2 comparison was virtually eliminated. While this new function shows promise of improving bulk model performance, it must be further validated before being accepted for universal application.

ACKNOWLEDGMENTS

This work was funded by the Office of Naval Research, Dr. Ron Ferek, program manager. The authors thank Keith Jones and Karl Gutekunst of the Naval Postgraduate School, Doug McKinney of McKinney Technology, and Michael Jablecki of SPAWAR Systems Center, San Diego, for their assistance in data collection.

REFERENCES

1. Andreas, E. L, "Estimating C_n^2 over snow and ice from meteorological data," *J. Opt. Soc. Am.*, **5A**, 481-495, 1988.

2. Fairall, C. W., E. F. Bradley, D. P. Rogers, J. B. Edson and G. S. Young, "Bulk parameterization of air-sea fluxes for Tropical Ocean-Global Atmosphere Coupled-Ocean Atmosphere Response Experiment," *J. Geophys. Res.*, **101**, 3747-3764, 1996.

3. Frederickson, P. A., K. L. Davidson, C. R. Zeisse, and C. S. Bendall, "Estimating the refractive index structure parameter (C_n^2) over the ocean using bulk methods," *J. Appl. Meteorol.*, **39**, 1770-1783, 2000.

4. Zeisse, C. R., B. D. Neener, and R. V. Dewees: "Measurement of low-altitude infrared propagation," *Appl. Opt.*, **39(6)**, 873-886, 2000.

5. Frederickson, P. A., S. Hammel, D. Tsintikidis, and K. Davidson, "Recent results on modeling the refractive-index structure parameter over the ocean surface using bulk methods," SPIE Conference on Atmospheric Optical Modeling, Measurement and Simulation, San Diego, CA, 2005.

6. Edson, J. B., and C. W. Fairall, "Similarity relationships in the marine atmospheric surface layer for terms in the TKE and scalar variance budgets," *J. Atmos. Sci.*, **55**, 2311-2328, 1998.